ISSN (ONLINE) 2583-2506
http://publications.rayatbahrauniversity.edu.in
RBIJMR-Rayat Bahra International Journal of Multidisciplinary Research, Vol. 02, Issue 01, June 2022

Impact Energy and Fracture Analysis of FDM Printed High Performance Nylon Composites

Irfan Yusuf[1], Aatif Haqani[2*], Varinder Singh[1] and Navjot Singh Mahal[1]

[1]Department of Mechanical Engineering, Rayat Bahra University, Mohali-140104, India
[2]Central Workshop, NIT Srinagar, Hazratbal-190006, India

Abstract: *This paper is aimed at studying and assessing the Impact Resistance and behaviour of the Fractured Surfaces of one of the most common and popular FDM engineering material (Nylon-6) and two of its composites (PACF and PAGF30). Charpy impact test using both U- and V-Notch specimens was carried out followed by SEM analysis of fractured surfaces. It was found that the Impact Strength of the Nylon Composites was higher than the neat nylon. The impact Energy absorbed by PAGF-30 was 18.6 % more than PACF and 210.56% more than PA6. The fractography of the fractured surfaces revealed that the main cause of failure of these materials is fiber pull-out, fiber breakage and matrix deformation and interface de-lamination.*

Keywords: Additive Manufacturing, FDM, 3D Printer, FRP, PA6, PACF, PAGF 30, Charpy Impact, SEM, Fractography

*Corresponding author: Irfan Yusuf
e-mail: irfaim66@gmail.com

ISSN (ONLINE) 2583-2506
http://publications.rayatbahrauniversity.edu.in
RBIJMR-Rayat Bahra International Journal of Multidisciplinary Research, Vol. 02, Issue 01, June 2022

1. Introduction

Rapid development and innovative advancements in extrusion-based 3D printing are changing the trajectory of Fused Deposition Modeling (FDM) technology. With increasing adoption across all industrial segments spanning from aerospace to automotive to healthcare, more and more industries are metamorphosing from metals to non-metals for the manufacturing of structural components, equipment parts, prototyping, tooling and implants. Perceptible to this transition, the materials used for FDM printing have also significantly evolved over the years, pushing materials science beyond the standard PLA and ABS filaments. From a wide array of selections, FDM users today can choose from composites, nylons, flexible, bio compatibles and engineering grade materials among many others. Our emphasis in this study is solely on high performance polyamide composites. Being cheap, light and faster to produce in smaller quantities, high performance polymers are outperforming their equivalent metal counterparts.

Composite materials are the blend of two or more different types of materials combined together to enhance the mechanical and structural properties of the end products. Composite materials augmented with fibers in a polymeric matrix are called as fiber-reinforced composites (FRP). FRP composites are used in diversified applications such as military vehicles, shelters, war fighting safety equipment, fighter aircrafts, naval ships, and submarine structures. These multidisciplinary fields of application make it necessary to understand and study various physical and mechanical properties of these materials when 3D printed [1, 2].

1.1 3D Printing a.k.a Additive Manufacturing (AM)

3D printing or additive manufacturing is the process of creating 3D solid objects from digital files. The creation of 3D printed objects is accomplished using an additive process. The additive process creates an object by overlaying successive layers of material until the object is created. Each of these layers can be viewed as thinly sliced cross-section of the object. From the context of this definition, Additive Manufacturing can be broadly divided into four stages as:

- Digital Modelling of the object to be created.
- Material(s) that combine the smallest possible shapes to form an object, such as a liquid drop, wire, or powder.

ISSN (ONLINE) 2583-2506
http://publications.rayatbahrauniversity.edu.in
RBIJMR-Rayat Bahra International Journal of Multidisciplinary Research, Vol. 02, Issue 01, June 2022

- 3D Printing Technique suitable for the selected material and its application thereby.
- Digital Control System to translate the sliced digital model into the exact motion of the 3D printing tool, laying the material layer-upon-layer to acquire the final desired shape and size.

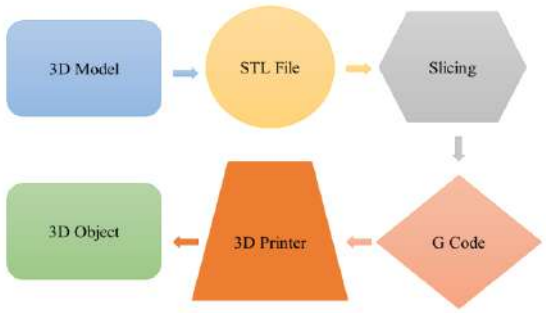

Fig. 1.: Workflow of 3D Printing Process

AM is thus fundamentally different from traditional formative or subtractive manufacturing in that it is the closest to the 'bottom up' manufacturing where we can build a structure into its designed shape using a 'layer-by-layer' approach [3]. This layer-by-layer manufacturing allows an unprecedented freedom in manufacturing complex, composite and hybrid structures with precision and control that cannot be made through traditional manufacturing routes [4]. In the last few decades, the AM has flourished in various fields such as aerospace industries for producing lightweight structures and complex cross-sectional areas like the honeycomb cell [5], architectural and automotive industries for prototype models [6], medical fields for prototype tissues and organs [7], and many other applications.

1.2 FDM (Fused Deposition Modeling) or FFF (Fused Filament Fabrication)

Fused deposition modeling (FDM), also known as fused filament fabrication (FFF), is an additive manufacturing process that falls within the category of material extrusion. In FDM, an object is built by selectively depositing melted material in a predetermined path, layer by layer. The materials used are thermoplastic polymers, which come in a filament form. FDM is the most widely used 3D printing technology. It comprises the largest installed base of 3D printers globally and is often the first 3D printing technology that people encounter.

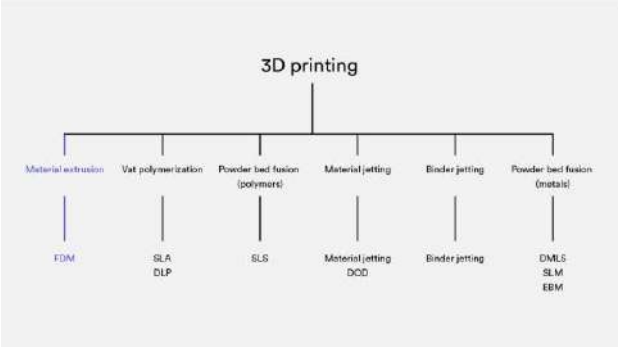

Fig. 2.: Various 3D Printing Technologies

ISSN (ONLINE) 2583-2506
http://publications.rayatbahrauniversity.edu.in
RBIJMR-Rayat Bahra International Journal of Multidisciplinary Research, Vol. 02, Issue 01, June 2022

The FDM fabrication process works by first loading a spool of thermoplastic filament into the printer.

Once the nozzle has reached the desired temperature, the filament is fed into the extrusion head and nozzle, where it melts. The extrusion head is attached to a three-axis system that allows it to move in the x-, y- and z-directions. Melted material is extruded in thin strands and deposited layer by layer in predetermined locations, where it cools and solidifies. Fans can be attached to the extrusion head to accelerate the cooling. To fill an area, multiple passes are required, similar to coloring in a rectangle with a marker. When a layer is finished, the build platform moves down (or in some machine setups, the extrusion head moves up) and a new layer is deposited. This process is repeated until the part is complete [8, 9].

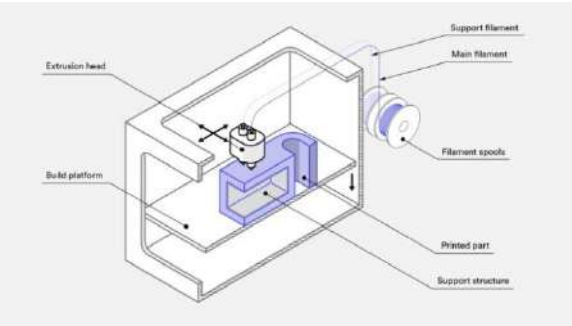

Fig. 3.: Schematic of a Typical FDM Printer

2. Materials and Methods

2.1 Material Selection

The materials used for 3D printing are as diverse as the products that result from the process. Initially, thermoplastic polymers such as Acrylonitrile butadiene styrene (ABS), Polylactic acid (PLA), polycarbonate (PC), polyamide (PA), Ultem and nylon were used as the feedstock in FFF-based 3D printing. Nevertheless, the products printed from pure thermoplastics show inferior mechanical properties in terms of strength and functionality in comparison to many load-bearing parts. These drawbacks restrict the FFF-printed neat polymer to be used for structural applications. As a result, FFF protocols need to be developed to print high-performance composite materials, particularly for load-bearing components.

In this study we chose to compare the difference between the following filaments: CarbonX™ Carbon Fiber Nylon (Gen3) 3D printing filament 1.75mm +/- 0.05mm in diameter with fibers 5-10 micrometers aligned following the axis of the material with the density of 1.17 g/cc, glass transition temperature of 70℃ and peak melting temperature of 265-285℃, AmideX™ PA6-GF30 Glass Fiber Nylon 3D printing filament 1.75mm +/- 0.05 mm in diameter with fibers made of glass reinforced into the polymer during manufacturing and aligned along the axis of filament with the density of 1.35 g/cc, glass

ISSN (ONLINE) 2583-2506
http://publications.rayatbahrauniversity.edu.in
RBIJMR-Rayat Bahra International Journal of Multidisciplinary Research, Vol. 02, Issue 01, June 2022

transition temperature of 70℃ and peak melting temperature of 260-280℃ and AmideX™ PA6 Copolymer 3D printing filament 1.75mm +/- 0.05 mm in diameter with the density of 1.12 g/cc, glass transition temperature of 76℃ and peak melting temperature of 270℃obtained from 3DXTECH, USA. The bulk mechanical properties of the materials were taken as mentioned in their respective datasheets.

2.2 Design and Manufacturing of Samples

The Specimens to be printed were designed (3D Modelled) using Solidworks according to the ASTM 5045 standards and then saved as .stl files (Fig. 4). The saved .stl files were then imported to superslicer ready to be sliced and loaded to the 3D printer for printing.

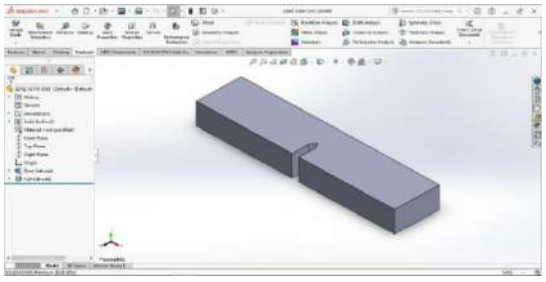

Fig. 4.: Specimen Model in Solid works

The enclosed Prusa Mini (Clone) 3D printer, based on the FFF principle was used to print the specimens. While printing the specimens, the print temperature, print speed and layer thickness were chosen according to the recommended settings by the filament manufacturer. All the FFF process parameters are summarized in the Table 1.

Table 1: Specimen Printing Parameters

Parameters	PA6	PA6-CF	PA6-GF3
Nozzle Size	0.4mm	0.4mm	0.4mm
Layer Height	0.25mm	0.25mm	0.25mm
Infill	100%, +/-45°	100%, +/-45°	100%, +/-45°
Extrusion Temp	270°C	275°C	265°C
Bed Temp	80°C	80°C	70°C
Specimen Orientation	XY Flat	XY Flat	XY Flat

3 samples of each material were FFF-printed to characterize the fracture plane and impact strength of U- and V-Notch specimens with dimensions 88 mm × 20 mm × 10 mm, based on the ASTM 5045 standard as shown in Fig. 5. The layers were printed in the XY plane whereas the build direction was along the Z-axis Fig. 6.

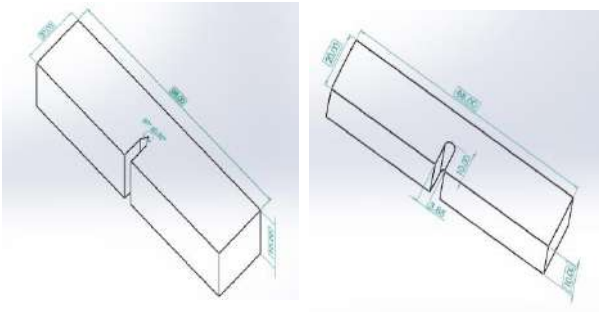

Fig. 5.: U- and V- Notch Specimen ASTM 5045

ISSN (ONLINE) 2583-2506
http://publications.rayatbahrauniversity.edu.in
RBIJMR-Rayat Bahra International Journal of Multidisciplinary Research, Vol. 02, Issue 01, June 2022

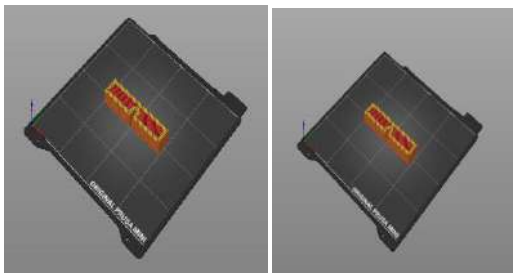

Fig. 6.: Specimen Sliced in Slicer Software

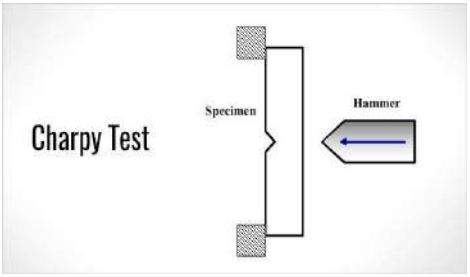

Fig. 7.: Charpy Impact Test Schematic

2.3 Experimental Setup

Each sample set consisted of three specimens for a given group of process parameters.Based on the mechanical test results, the mean impact strength values were calculated. Since the physical properties of the thermoplastics is highly dependent on the ambient temperature, the tests were performed at the room temperature according to the standards.

Fig. 6: Test Specimens U and V Notch

Charpy Impact Test was performed to determine the amount of energy absorbed by the specimen during fracture followed by the SEM analysis of the fractured surfaces.

The Impact tests were performed on the Walter + Bai ag CHV Expandable Motorized pendulum Impact Tester PH 400 Joule. This sophisticated apparatus takes the angle of fall of the pendulum as the input value and displays the output on the display after the fracture automatically with the help of a patented laser opto-electronic-measuring-system. The angle of fall of the pendulum was kept at 120° for all test specimens. Also the energy dissipated due to air resistance was measured to be 1.8 J.

3. Results and Discussion

3.1 Impact Energy Analysis

The Impact Test of the specimens was performed in conformance with the ASTM E-23 standards. Both U- and V-Notch test specimens of dimensions 88mm x 20mm x 10mm were tested in the same conditions with a constant impact angle of 120°. Chart 1. shows the Average Impact Energy (in J) of the specimens. As observed from the plot, the PA-GF30

ISSN (ONLINE) 2583-2506
http://publications.rayatbahrauniversity.edu.in
RBIJMR-Rayat Bahra International Journal of Multidisciplinary Research, Vol. 02, Issue 01, June 2022

specimens showed the maximum impact strength of the three materials followed by the PA-CF and PA6. The average impact energy of PA-GF30 V-Notch specimen is 94.1 J which is 18.66% more than PA-CF and 210.56% more than PA6.

Fig. 8: Impact Testing Machine

This could be due to the ductile nature of the glass fiber absorbing more energy [10]. Same trend of energy absorption is seen in U-Notch specimens as well with PA-GF30 absorbing more energy before failure followed by PA-CF and PA6. However, the energy absorption of U-Notch specimens is more than the corresponding V-Notch specimens.

Charts 2, 3 and 4 show the Impact Energy Distribution Plots of the three samples of each specimen. Each box shows the minimum value, the first quartile, the median, the second quartile and the maximum value of Impact Energy absorbed by each specimen. There is a uniform distribution of the values about the median in all of the specimens with V-Notch specimens showing more scattering about the median as compared to the U-Notch specimens.

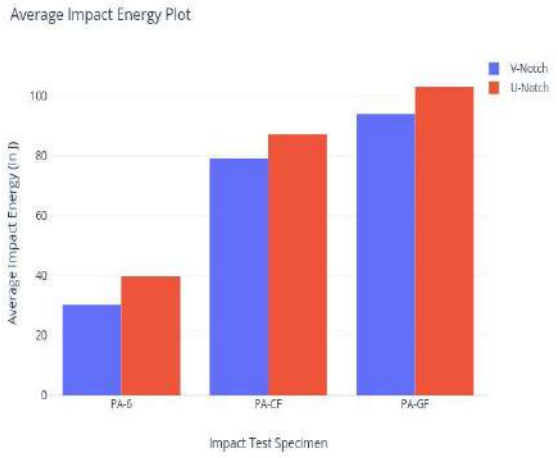

Chart 1.: Average Impact Energy Plot of different specimens

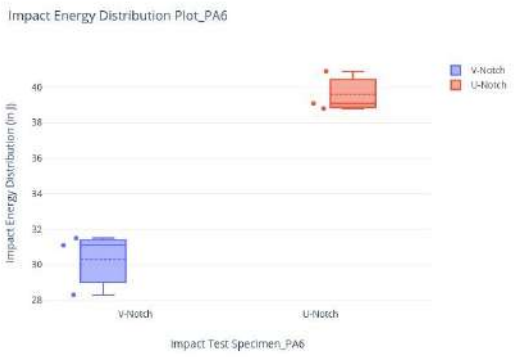

Chart 2.: Impact Energy Distribution Plot PA6

ISSN (ONLINE) 2583-2506
http://publications.rayatbahrauniversity.edu.in
RBIJMR-Rayat Bahra International Journal of Multidisciplinary Research, Vol. 02, Issue 01, June 2022

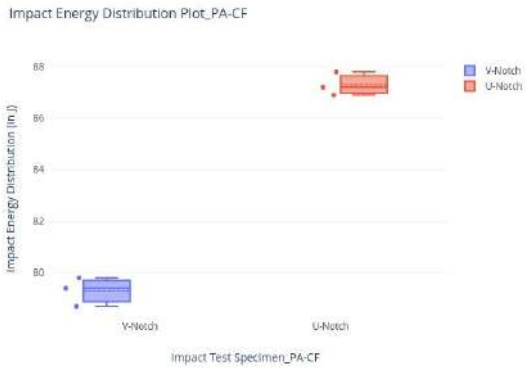

Chart -3: Impact Energy Distribution Plot PA-CF

Chart -4: Impact Energy Distribution Plot PA-GF30

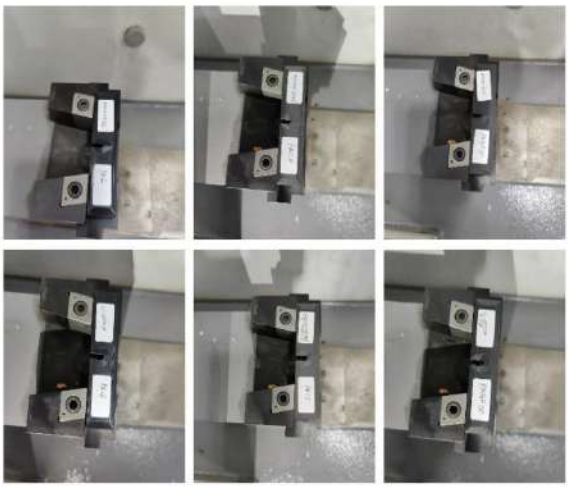

Fig. 9: Specimens Loaded in the Testing Machine

3.2 Fracture Analysis

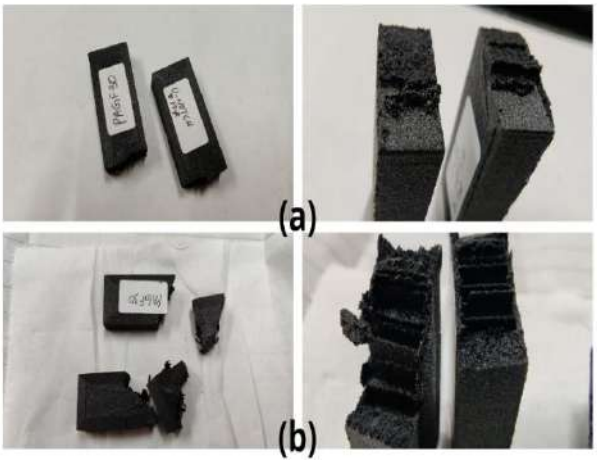

Fig. 10: Fractured Specimen (a) PA-GF30 U-Notch (b) PA-GF30 V-Notch

Fig -10 shows the U- and V – Notch PA-GF30 specimens after Impact Fracture. The U-Notch specimen has a continuous propagation of the crack along the direction of the impact with a smooth fracture surface formation and no delamination of the layers, while as the V-Notch specimen is broken into pieces and the crack propagation is irregular resulting in an uneven

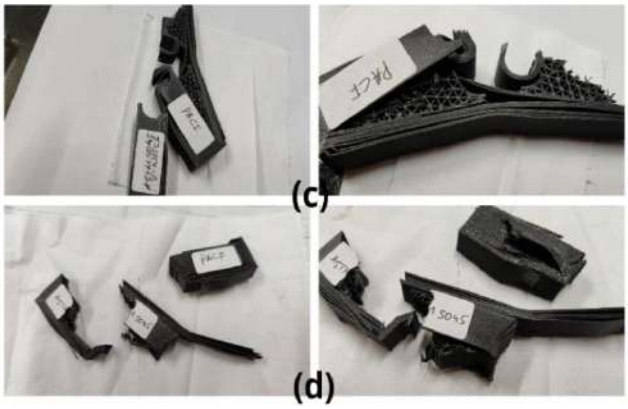

Fig. 11: Fractured Specimen (a) PA-CF V-Notch (b) PA-CF U-Notch

ISSN (ONLINE) 2583-2506
http://publications.rayatbahrauniversity.edu.in
RBIJMR-Rayat Bahra International Journal of Multidisciplinary Research, Vol. 02, Issue 01, June 2022

fracture surface though again no delamination of the layers can be seen.

Fig. 11 shows the fractured U- and V – Notch specimens of PA-CF. The fracture behavior of this particular specimen is completely different. As can be seen from figure (c), the specimen didn't break all the way along the direction of the impact like PA-GF30, instead the layers were teared away, walls de-laminated and deformed. On the other hand, the V-Notch specimen broke all the way through all the layers and the resulting impact damage can be seen on the opposite face of one of the broken pieces of the specimen indicating a brittle fracture.

Fig. 12: Fractured Specimen (a) PA6 V-Notch (b) PA6 U-Notch

Fig. 12. shows that U- and V-Notch PA6 specimens whose fracture surface is surprisingly same as that of the PA-GF30 but with much lower impact strength.

3.2 SEM Micrographs of Fractured Surfaces

SEM analysis was performed on one sample cut 10mm away from the fracture surface from each material. The fracture surfaces of the samples were coated with gold prior to SEM analysis because of their non-conductive nature. Hitachi 3600 N Scanning electron microscope with a 5-axis motorized stage coupled with ultra-dry Compact EDS Detector (Thermo Scientific™) was used for high resolution imaging and elemental analysis of the filament samples used for making the specimens to qualitatively identify the void contents and understand the inter-bead bonding surface.

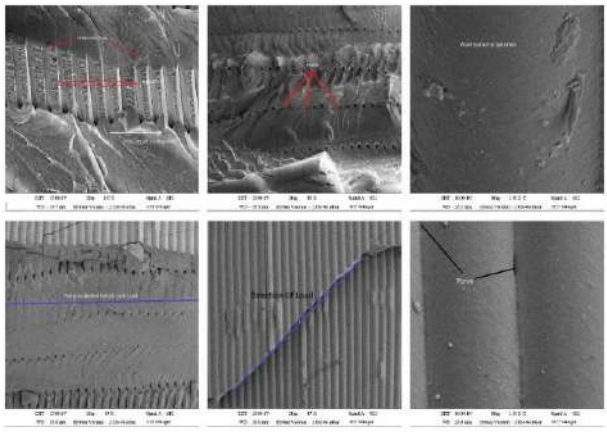

Fig. 13: SEM micrographs of PA6 U- and V-Notch Specimens

ISSN (ONLINE) 2583-2506
http://publications.rayatbahrauniversity.edu.in
RBIJMR-Rayat Bahra International Journal of Multidisciplinary Research, Vol. 02, Issue 01, June 2022

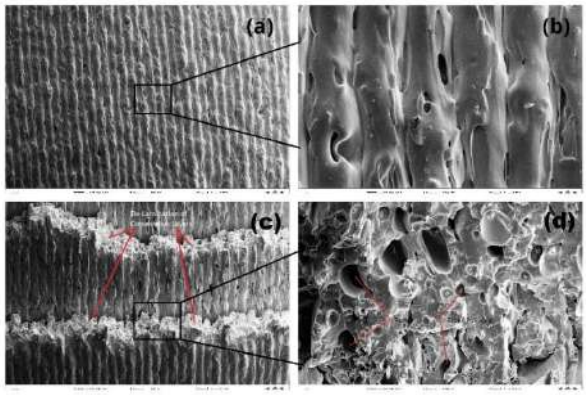

Fig. 14: SEM micrographs of (a) PA-CF V-Notch fractured surface showing delamination of the top layer (b) magnified view of the zone showing good transverse layer adhesion and pores (c) PA-CF U-Notch surface with de-lamination and tearing (d) magnified view of the surface showing porosity, fiber pull-out, broken fibers and brittle fracture.

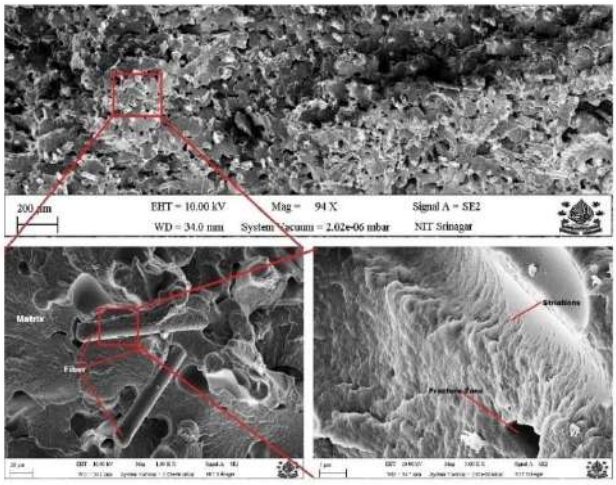

Fig. 15: SEM micrographs showing the fracture surface of PA-GF30 U-Notch specimen in 200µm, 20µm and 5µm.

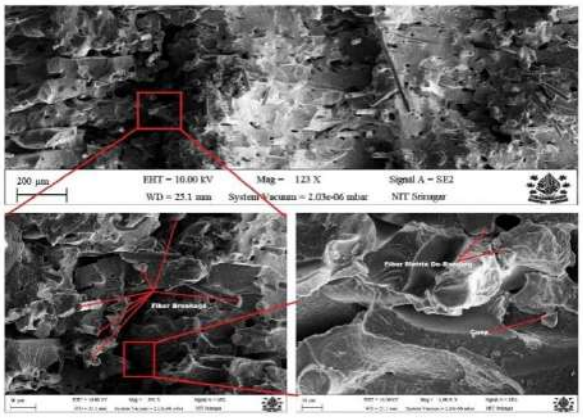

Fig. 16: SEM micrographs showing the fracture surface of PA-GF30 V-Notch specimen in 200µm, 50µm and 10µm.

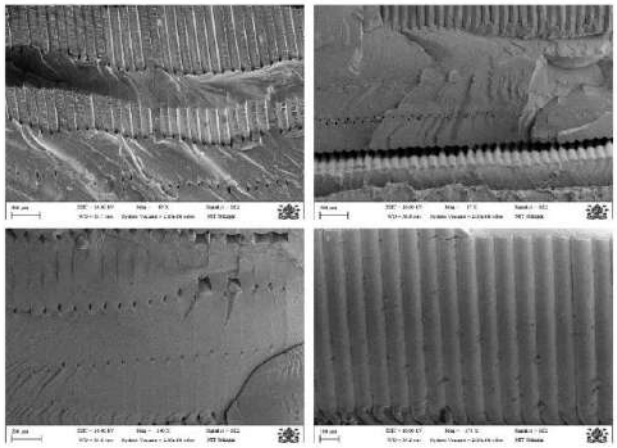

Fig. 17: SEM Images of the PA6 Specimens showing good layer adhesion, Uniform crack front, layer stacking with voids and classical River and Hackle Lines.

ISSN (ONLINE) 2583-2506
http://publications.rayatbahrauniversity.edu.in
RBIJMR-Rayat Bahra International Journal of Multidisciplinary Research, Vol. 02, Issue 01, June 2022

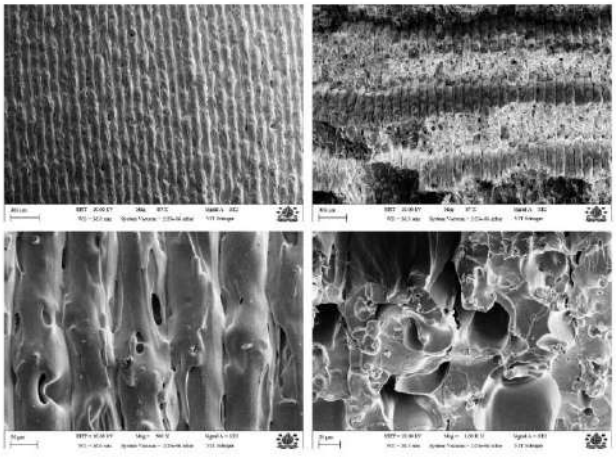

Fig. 18: SEM Images of the PA-CF Specimens showing over-lapping layer stacks, micro pores, serrated fracture surface and dominant de-lamination failure.

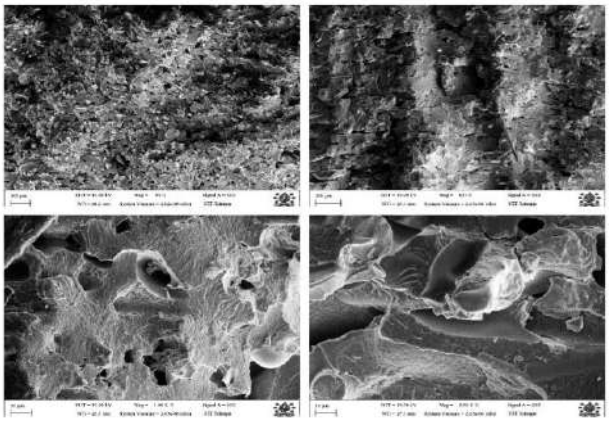

Fig. 19: SEM Images of the PA-GF30 Specimens showing Fiber Breakage, Fiber Pull-out, Matrix Cracking and de-bonding.

3. Conclusions

This study dealt with the impact strength and fracture analysis of neat Nylon (PA6) and its two most common composites PA-CF (Carbon Fiber Filled) and PA-GF30 (30% Glass Fiber Filled). Charpy tests were performed on the U- and V-Notch specimens of these materials to determine their Impact Resistance which was then followed by the fractography of the fractured surfaces of the specimens using SEM.

Analysis of the fracture surfaces of neat nylon and both of its fiber-reinforced composites showed that failure was mainly caused by fiber pull-out, fiber breakage and delamination, whereas void formation within the structure was the cause of failure. It turns out that it acts as a weak point. Fiber pull-out occurs due to poor adhesion between the matrix and the fibers. Voids can occur within the structure being printed or within the fiber reinforced filaments. Surface roughness is caused by line-by-line deposition and the staircase effect by layer-upon-layer deposition. These are the most common drawbacks of FDM printed parts.

References

[1] Rajak, Dipen Kumar, Durgesh D. Pagar, Pradeep L. Menezes, and Emanoil Linul. (2019), Fiber-Reinforced Polymer Composites: Manufacturing, Properties, and Applications, Polymers, **11 (10)**, pp.1667; https://doi.org/10.3390/polym11101667.

[2] T., S., P., S. and M. S., A. (2020), A review on advancements in applications of fused deposition modeling process, Rapid Prototyping Journal, **26 (4)**, pp.669-687; https://doi.org/10.1108/RPJ-08-2018-0199.

[3] A. M. Syed, Tofail, Elias P. Koumoulos, Amit Bandyopadhyay, Susmita Bose, Lisa O'Donoghue and Costas Charitidis, (2018), Additive manufacturing: scientific and technological challenges, market uptake and opportunities, Materials Today, **21 (1)**, pp.22-37; https://doi.org/10.1016/j.mattod.2017.07.001 .

[4] A. Bandyopadhyay, S. Bose, "Additive Manufacturing", CRC Press, Florida (2015). https://doi.org/10.1016/j.addma.2020.101241 .

[5] Mohammad Arif, Mohammad Asif, and Israr Ahmed, (2017), Advanced Composite Material for Aerospace Application: A Review, Int. J. Engg. and Manufacturing Science, **7 (2)**, pp. 393-409. https://ripublication.com/ijems17/ijemsv7n2_21.pdf.

[6] I. Gibson, D. W. Rosen and B. Stucker, (2009), Additive Manufacturing Technologies: Rapid Prototyping to Direct Digital Manufacturing, Springer, Berlin.

[7] P. Jain, H. Kathuria and N. Dubey, (2022), Advances in 3D bioprinting of tissues/organs for regenerative medicine and in-vitro models, Biomaterials; https://doi.org/10.1016/j.biomaterials.2022.121639.

[8] The Types of 3D Printing Technology of 2021 | All3DP.

[9] S. Vyavahare, S. Teraiya, D. Panghal, and S. Kumar, (2020), Fused deposition modelling: a review, Rapid Prototyping Journal, **26 (1)**, pp.176-201; https://doi.org/10.1108/RPJ-04-2019-0106.

[10] P. R. S. Reddy, T. S. Reddy, K. Mogulanna, I. Srikanth, V. Madhu and K.V. Rao, (2017), Procedia Engg., **173**, pp.293-298;https://doi.org/10.1016/j.promfg.2018.02.079.